Identification of domains in apoA-I susceptible to proteolysis by mast cell chymase: implications for HDL function

Miriam Lee,[1,*] Patrizia Uboldi,[†] Daniela Giudice,[†] Alberico L. Catapano,[†,§] and Petri T. Kovanen[2,*]

Wihuri Research Institute,* Kalliolinnantie 4, Helsinki 00140, Finland, and Institute of Pharmacological Sciences,[†] and Centro per lo Studio dell'arteriosclerosi,[§] University of Milan, Italy

Abstract When stimulated, rat serosal mast cells degranulate and secrete a cytoplasmic neutral protease, chymase. We studied the fragmentation of apolipoprotein (apo) A-I during proteolysis of HDL_3 by chymase, and examined how chymase-dependent proteolysis interfered with the binding of eight murine monoclonal antibodies (Mabs) against functional domains of apoA-I. Size exclusion chromatography of HDL_3 revealed that proteolysis for up to 24 h did not alter the integrity of the α-migrating HDL, whereas a minor peak containing particles of smaller size with preβ mobility disappeared after as little as 15 min of incubation. At the same time, generation of a large (26 kDa) polypeptide containing the N-terminus of apoA-I was detected. This large fragment and other medium-sized fragments of apoA-I produced after prolonged treatment with chymase were found to be associated with the αHDL; meanwhile, small lipid-free peptides were rapidly produced. Incubation of HDL_3 with chymase inhibited binding of Mab A-I-9 (specific for $preβ_1$HDL) most rapidly (within 15 min) of the eight studied Mabs. This rapid loss of binding was paralleled by a similar reduction in the ability of HDL_3 to induce high-affinity efflux of cholesterol from macrophage foam cells, indicating that proteolysis had destroyed an epitope that is critical for this function. In sharp contrast, prolonged degradation of HDL_3 by chymase failed to reduce the ability of HDL_3 to activate LCAT, even though it led to modification of three epitopes in the central region of apoA-I that are involved in lecithin cholesterol acyltransferase (LCAT) activation. This differential sensitivity of the two key functions of HDL_3 to the proteolytic action of mast cell chymase is compatible with the notion that, in reverse cholesterol transport, intactness of apoA-I is essential for $preβ_1$HDL to promote the high-affinity efflux of cellular cholesterol, but not for the α-migrating HDL particles to activate LCAT.—Lee, M., P. Uboldi, D. Giudice, A. L. Catapano, and P. T. Kovanen. **Identification of domains in apoA-I susceptible to proteolysis by mast cell chymase: implications for HDL function.** ***J. Lipid Res.*** 41: **975–984.**

Supplementary key words α- and preβ-migrating HDL • monoclonal antibodies • LCAT • cellular cholesterol efflux • proteolysis of apoA-I

A negative association between plasma levels of cholesterol in high density lipoproteins (HDL) and the risk of coronary heart disease is well established (1). The involvement of HDL in the prevention and regression of atherosclerosis has been mainly associated with two functions: *a*) the ability of HDL to act as cellular cholesterol acceptors, and *b*) the ability of HDL to esterify cholesterol in plasma through the activation of lecithin cholesterol acyl transferase (LCAT) (2). Both functions of HDL are critical for the removal of cellular cholesterol and its subsequent metabolism by the liver. The role of HDL in this process of reverse cholesterol transport has been related to their content and specific domains in apoA-I, their main apolipoprotein.

HDL are heterogeneous, the various subclasses of HDL particles differing in size, chemical composition, and immunological response (3). Most HDL are spheroidal particles displaying α-mobility in agarose gels with a core composed largely of esterified cholesterol; however, some HDL species do not contain core lipids and have preβ electrophoretic mobility. Although precise characterization of the latter has not been achieved, three size subclasses of preβHDL have been described: $preβ_1$, which are the smallest and contain only one molecule of apoA-I; $preβ_2$, which are phospholipid-rich discs containing three apoA-I molecules; and $preβ_3$ which, in addition to apoA-I, contain LCAT and cholesteryl ester transfer protein (2). PreβHDL, unlike some of the αHDL, do not contain apoA-II (2). In plasma, the various HDL particles are in a

Abbreviations: apoA-I, apolipoprotein A-I; Mab, monoclonal antibody; LCAT, lecithin cholesterol acyltransferase; HDL_3, high density lipoproteins$_3$; PBS, phosphate buffered saline; BSA, bovine serum albumin; FFA, free fatty acid; DMEM, Dulbecco's modified Eagle's medium; TLC, thin-layer chromatography; BTEE, N-benzoyl-L-tyrosine ethyl ester; AP, alkaline phosphatase; pNPP, p-nitrophenyl phosphate; TCA, trichloroacetic acid; SDS, sodium dodecyl sulfate; PAGE, polyacrylamide gel electrophoresis; 2D-PAGGE, two dimensional polyacrylamide gradient gel electrophoresis; LpA-I, lipoproteins containing apoA-I; ELISA, enzyme linked inmunosorbent assay; LCAT, lecithin cholesterol acyltransferase.

[1] Present address: Faculty of Biology, University of Havana, Vedado, Havana, Cuba.

[2] To whom correspondence should be addressed.

dynamic state of precursor-product relationship and play different roles in reverse cholesterol transport. Indeed, the lipoprotein particles in the smallest preβ-migrating HDL subpopulation have been demonstrated to act as the earliest acceptors of cholesterol from cell membranes (4). After cholesterol has been taken up by these acceptors, the activation of LCAT plays an important role in the clearance of excess cholesterol from peripheral cells to the liver, as this enzyme allows channeling of cholesterol from the initial acceptors to the spherical α-migrating HDL, leading to maturation of the HDL particles.

We have studied the effect of the neutral protease chymase present in exocytosed rat mast cell granules (i.e., granule remnants) on the functional modification of HDL. These studies disclosed that degradation of HDL_3 or LpA-I by granule remnant chymase efficiently blocks the high-affinity efflux of cholesterol from macrophage foam cells promoted by these acceptors (5, 6). Moreover, our most recent results demonstrated that, when lipid-free apoA-I or apoA-I-containing acceptors (plasma or HDL_3) were incubated with chymase of rat or human origin and added to macrophage cell cultures, the mechanism responsible for the observed reduction in cholesterol efflux was selective depletion of $preβ_1$LpA-I particles, as observed in 2D-PAGGE (7). The precise mechanism by which structural modification of proteolyzed apoA-I leads to the functional changes described above is not known. However, the results strongly suggested that heterogeneity of apoA-I fragmentation had occurred among the different subclasses of HDL present in the incubation system.

The conformation of apoA-I in HDL required for full or specific biological activity of the lipoprotein has been studied by different methods such as site-directed mutagenesis, or by using synthetic peptides or monoclonal antibodies for epitope mapping (for review, see ref. 8). These studies have defined regions in apoA-I which appear to be structurally and functionally distinct. It has been observed that specific domains determine the lipid-binding properties of apoA-I (9), the interaction of apoA-I with plasma membranes (10, 11), the ability of apoA-I to induce cellular cholesterol efflux (12–16), and the ability of apoA-I to activate LCAT (17–22). Thus, it may be possible that proteolysis of apoA-I in $preβ_1$HDL by mast cell granule remnants disrupts the assembly of these particles and destroys structural domains in apoA-I that are required for promoting the high-affinity efflux of cellular cholesterol. It is also possible that proteolytic modification of apoA-I, not only in preβ-migrating HDL, but also in α-migrating species of HDL, may alter other biological functions of these lipoproteins, such as LCAT activation.

To gain further insight into the specific degradation of apoA-I in HDL_3 by chymase, we examined this apolipoprotein for fragmentation and loss of specific epitopes when subjected to proteolysis by granule remnants, and related the observed changes to two functions of apoA-I in HDL, namely the induction of cholesterol efflux from macrophage foam cells and the activation of LCAT.

METHODS

Animals

Adult male Wistar rats and female NMRI mice were purchased from the Viikki Laboratory Animal Center, University of Helsinki.

Isolation of rat mast cell granule remnants

Serosal mast cells were isolated from the peritoneal and pleural cavities of rats. Degranulation was induced with compound 48/80 (Sigma) and the exocytosed granules, i.e., granule remnants, were isolated from the released material by centrifugation as described (23). The quantity of granule remnants is expressed in terms of their total protein content (24) or of their proteolytic activity with BTEE as substrate (25), as previously described (26). This isolation procedure does not release chymase from the heparin glycosaminoglycan chains of granule remnants. Hence, reference to "chymase" or to "granule remnants" denotes the fully active chymase associated with the granule remnant heparin proteoglycan matrix (6).

Isolation of plasma lipoproteins

Human LDL (d 1.019–1.050 g/mL) and HDL_3 (d 1.125–1.210 g/mL) were isolated from fresh normolipidemic plasma by sequential ultracentrifugation, using KBr (27). The quantities of the lipoproteins are expressed in terms of their protein content (24). We have observed that this ultracentrifugally isolated HDL_3 fraction contains both α- and preβ-migrating HDL (7, 28).

Chemical modification and radioactive labeling of lipoproteins

LDL was acetylated (acetyl-LDL) by repeated additions of acetic anhydride (29). Acetyl-LDL, radiolabeled by treatment with [^{3}H]cholesteryl linoleate (1,2(n)[^{3}H]cholesteryl linoleate, Amersham International) dissolved in 10% dimethylsulfoxide (30), yielded preparations of [^{3}H]cholesteryl linoleate bound to acetyl-LDL with specific activities ranging from 30 to 100 $\times$ 10^3 dpm/μg protein. HDL_3 was iodinated with ^{125}I (Na^{125}I, Amersham International) by the iodine monochloride method as described (31, 32).

Monoclonal antibodies

The eight murine Mabs used in this work were a kind gift from Dr. S. Marcovina, and have been described and characterized previously, namely A-I-9 and A-I-15 were shown to recognize specific epitopes of preβHDL species (15), and A-I-5, A-I-8, A-I-11, A-I-16, A-I-19, and A-I-57 were tested for their capacity to identify the apoA-I epitopes involved in the activation of LCAT (22). A-I-19 recognizes the N-terminal fragment of apoA-I, while the other Mabs recognize different epitopes in the central region of apoA-I, between residues 93 and 174. Four of these Mabs bind epitopes in apoA-I that are involved in the activation of LCAT. The main characteristics of the set of Mabs are summarized in **Table 1**.

Proteolysis of HDL_3 by chymase in granule remnants

HDL_3 (1 mg/mL) was incubated at 37°C in 1 mL of 150 mM NaCl, 1 mM EDTA, 5 mM Tris-HCl, pH 7.4, in the absence or presence of granule remnants (30 μg total protein equal to 40 BTEE units of chymase) for different periods of time. At the end of the incubations, the granule remnants were sedimented by centrifuging the reaction mixtures at 4°C, 15,000 rpm for 5 min, and aliquots of the supernatants were taken for the following assays: *a*) analysis of degradation products of apoA-I in SDS-PAGE, and gel filtration of the proteolyzed HDL_3 preparation, *b*) binding of anti-apoA-I monoclonal antibodies to apoA-I in chymase-treated HDL_3 by direct ELISA, *c*) induction of cholesterol efflux

TABLE 1. Immunoreactivity of anti-apoA-I monoclonal antibodies and their ability to block the LCAT reaction

Monoclonal Antibody	Epitope Recognized in apoA-I[a]	Lipoprotein Specificity	Ability to Block LCAT Activation
A-I-5	133–141	HDL	+
A-I-8	144–148	HDL	+
A-I-9	137–144	preβ_1HDL	ND
A-I-11	124–128	HDL	−
	144–148 (minor)		
A-I-15	93–99	preβ_2HDL	ND
A-I-16	144–148	HDL	+
	124–128 (minor)		
A-I-19	1–10	HDL	−
A-I-57	167–174	HDL	+

ND = not determined.

[a] Note that all monoclonal antibodies recognize epitopes in the central region of apoA-I (full length: 1–243) except A-I-19, which recognizes the N-terminal region.

from cultured mouse macrophage foam cells by chymase-treated HDL_3, and *d*) promotion of cholesterol esterification by chymase-treated HDL_3 via activation of LCAT. The degree of proteolysis was estimated by measuring the generation of small peptides by incubation of ^{125}I-labeled HDL_3 (1 mg/mL, 200 cpm/μg) with granule remnants in the conditions described above. After the indicated time periods, the incubation mixtures were treated with 10% TCA to determine the amount of small peptides soluble in TCA. The values of ^{125}I-labeled HDL_3 degradation (i.e., generation of TCA-soluble radioactivity) are expressed as percentages of the total radioactivity present at the start of incubation. The digestion products of apoA-I were also analyzed by SDS-PAGE as described below.

SDS-PAGE of apoA-I proteolytic products

In order to study the proteolytic products of apoA-I after digestion with granule remnant chymase, aliquots of the above supernatants were analyzed by SDS gel electrophoresis in 15% polyacrylamide gel according to Weber and Osborn (33), using a Bio-Rad minicell (Bio-Rad, Richmond, CA) and Bio-Rad broad-range MW standards. After electrophoresis, the peptide bands in the gels were either visualized with Coomassie Blue or transferred to a nitrocellulose membrane (34). Immunoblotting of the gels was performed utilizing an anti-human apoA-I polyclonal antibody (Behring), or the set of Mabs to visualize the bands. Immunocomplexes were detected by an enhanced chemiluminescence method (ECL, Amersham) followed by autoradiography according to the manufacturer's instructions. The time course of the disappearance of apoA-I from HDL_3 treated with chymase was also evaluated by scanning of gels after Coomassie Blue staining in a LKB Ultroscan XL densitometer. The mean of the area corresponding to apoA-I in three different gels was expressed as a percentage of control samples incubated in parallel without granule remnants, which were taken as 100%.

Fractionation of HDL_3 by size exclusion chromatography

In order to analyze the effect of proteolysis on the size and homogeneity of the lipoprotein particles contained in the HDL_3 fraction, native HDL_3 and HDL_3 incubated in the absence or presence of granule remnant chymase for 15 min or 24 h were passed through a Superose 12 (Prepacked HR 10/30 column, Amersham Pharmacia Biotech) at room temperature using a solution of 150 mM NaCl, 1 mM EDTA, 5 mM Tris-HCl, pH 7.4 as eluant at a flow rate of 0.4 mL/min. After excluding the void volume, fractions were collected and monitored by continuously measuring the OD_{280}, data was automatically recorded in an interfaced computer device (SMART, Pharmacia LKB). The column was standardized with the following molecular mass standards (MW standard Bio-Rad): thyroglobulin 670 kDa (elution at 8.5 mL), gamma globulin 158 kDa (11.2 mL), ovalbumin 44 kDa (13 mL), myoglobin 17 kDa (14.5 mL), and vitamin B-12 1.3 kDa (19.2 mL). Fractions containing the main peak of HDL (peak I) and minor peaks (peaks II and III) eluted from the column. These fractions were correspondingly pooled, concentrated by centrifuging the samples in a vacuum, and de-salted by dialysis on Millipore membranes (0.025 μm) for further analysis.

ELISA assay to study the interaction of monoclonal antibodies with chymase-treated HDL_3

To study the binding of Mabs to the apoA-I in chymase-treated HDL_3, a previously described direct ELISA procedure was adapted. For this purpose, microtiter plates were coated overnight with 5 μg/mL of control HDL_3 or of chymase-treated HDL_3. After washings (PBS-Tween 0.05% × 3, PBS × 1), nonspecific binding sites were saturated with PBS-BSA 3%, followed by another cycle of washings. Fifty microliters of Mab anti-apoA-I appropriately diluted with precoating buffer was added to each set of wells, and the plates were incubated for 2 h at room temperature with shaking. After washings, the plates were incubated for 1 h with 50 μL of alkaline phosphatase (AP)-conjugated anti-mouse IgG (1:1000), 50 μL of substrate for AP (pNPP) were added, and the OD 405 nm was read when enough color had developed (usually 30 min) in a plate reader.

Cholesterol efflux assay

Peritoneal cells were harvested from unstimulated mice in PBS containing 1 mg/mL BSA. The cells were recovered after centrifugation and resuspended in DMEM (GIBCO) with 100 U/mL penicillin and 100 μg/mL streptomycin (medium A) supplemented with 20% fetal calf serum, and plated into 24-well plates (Becton Dickinson Labware). After incubation at 37°C for 2 h in humidified CO_2, nonadherent cells were removed. After washing with PBS, the adherent cells (macrophages) were loaded with [^{3}H]cholesterol by incubation for 18 h in the presence of 20 μg/mL of [^{3}H]cholesteryl linoleate acetyl-LDL in medium A containing 20% fetal calf serum. [^{3}H]cholesterol-loaded macrophages were washed with PBS and incubated with fresh medium A containing 50 μg/mL of HDL_3. After 6 h, the media were collected and centrifuged at 200 *g* for 5 min. The radioactivity in each supernatant was determined by liquid scintillation counting. Under the conditions used, [^{3}H]cholesterol efflux is linear up to 6 h of incubation with foam cells (6). The experimental data points are means of triplicate measurements.

Isolation of LCAT

LCAT was partially purified as previously described (35). In brief, 20 mL of dextran sulfate (MW 50,000, 10 g/L, 500 mM $MgCl_2$) were slowly added to 200 mL of plasma with continuous stirring at 4°C. The mixture was incubated for 10 min and then centrifuged at 2500 rpm at 4°C for 30 min. The supernatant was taken, 11.6 g of solid NaCl was added and dissolved, and applied to a phenyl-Sepharose column. The column was eluted with distilled water and the fractions containing LCAT activity were collected and pooled, dialyzed against 20 mM sodium phosphate buffer, pH 7.1, and passed through a Protein A-Sepharose (Affi-Gel Blue column, Bio-Rad, Richmond, CA). LCAT activity was eluted with phosphate buffer (20 mM, pH 7.1) and the partially purified enzyme was stored at −80°C until use. Absence of apoA-I in the partially purified LCAT preparation was confirmed by immunoassay for apoA-I detection after PAGE.

Cholesterol esterification assay

Cholesterol esterification was measured as described (36) with the following modifications. The substrate mixture to determine LCAT activity was prepared by adding 25 μL of a solution of radioactive cholesterol (21.6 μL [^{3}H]cholesterol, specific activity 5.1 Ci/mM, in 4 mL of 2% BSA-FFA) to aliquots of HDL_3 containing 4 μg of cholesterol in a final volume of 460 μL of 10 mM Tris, 140 mM NaCl, 1 mM EDTA, pH 7.4. The mixture was allowed to stand in a cold room for 4 h and 25 μL of 100 mM β-mercaptoethanol was added together with 15 μL of purified LCAT. The assay mixture, which contained 0.135 μCi (0.026 nmol) of [^{3}H]cholesterol, was incubated overnight at 37°C. The reaction was stopped by addition of 2 mL of ethanol and the bottom phase was extracted twice with 3 mL of hexane. The extracts were collected, dried under nitrogen, and dissolved in 250 μL of chloroform. Aliquots were applied to TLC in petroleum ether–diethyl ether–acetic acid 70:30:1 (v/v/v) as running solvent mixture, and the radioactivities associated with free cholesterol and esterified cholesterol were determined by liquid scintillation counting. In a preliminary set of experiments, conditions were set up in which 50% of maximal esterification was obtained. Therefore, under the experimental conditions, any cleavage of apoA-I or modification in its conformation that changed the ability of the apolipoprotein to activate LCAT, would be detected. In this assay with [^{3}H]cholesterol-labeled HDL_3 of relatively low specific activity, long incubation times were used to obtain high enough substrate conversion, and, therefore, high enough quantities of radioactivity for reliable counting of the reaction product. The rate of cholesterol esterification was linear for at least 24 h, and therefore, the values at 24 h gave an estimate of the constant reaction rate during this period of time.

Other assays

Agarose electrophoresis was performed in the Beckman Paragon Lipokit, staining the gels with Coomassie Blue. The phospholipid content was measured using a commercial kit (BioMerieux S.A., France).

RESULTS

Fragments generated from apoA-I by treatment of HDL_3 with granule remnants

In the early studies on HDL_3 degradation by mast cell granule remnant chymase, we observed that incubation of 1 mg of ^{125}I-labeled HDL_3 in the presence of a large quantity of granule remnants (170 μg) resulted in rapid degradation of apoHDL (5), producing approximately 12% of TCA-soluble peptides after incubation for 2 h at 37°C. To produce a slower rate of degradation of HDL_3 by chymase, we now added 30 μg of granule remnants to 1 mg of HDL_3. This was done in an attempt to induce a slow and progressive modification of epitopes of apoA-I. Under these conditions, generation of 13% of TCA-soluble peptides was observed after incubation for 24 h. With shorter treatment times (15 and 30 min), proteolysis by chymase generated less than 3% of TCA-soluble peptides from apoHDL_3 (**Fig. 1**).

Analysis of the course of the proteolysis by SDS-PAGE showed that incubation of HDL_3 with granule remnant chymase produced one polypeptide fragment of 26 kDa which appeared in Coomassie Blue-stained gels after the shortest incubation period (15 min). To obtain strong staining of this fragment, a gel was overloaded with HDL_3 (**Fig. 2, panel A**; uppermost gel, shown by an arrow). This band was recognized by a polyclonal anti-apoA-I after blotting of the gels and remained visible during the entire course of hydrolysis with chymase, as shown in panel A. In order to identify whether the cleavage occurred in the C- or the N-terminus of apoA-I and to obtain more information on the sequences contained in the polypeptides produced by digestion with chymase, we used monoclonal site-specific apoA-I antibodies. Thus, immunostaining with antibody A-I-19 (epitope between residues 1 and 10) revealed that the 26 kDa fragment contained the N-terminus of apoA-I, and the band was also recognized by A-I-57, the monoclonal antibody closer to the C-terminus (panel A). As this large fragment (26 kDa) contained the N-terminus of apoA-I, the first cleavage had occurred in the C-terminal region. The absolute amount of apoA-I in HDL_3 degraded by chymase was also evaluated densitometrically, by measuring the progressive disappearance of the apoA-I band in Coomassie Blue-stained SDS-PAGE gels after treatment with chymase. Using this approach, the average degradation of apoA-I (in three SDS-PAGE gels) was less than 10% during incubations for 15 to 30 min, and 14 and 29% after 6 and 24 h of incubation, respectively (note that the gel shown in panel A has been overloaded to better visualize the otherwise faint 26 kDa band). No apparent decrease in the apoA-II band was observed upon incubation of HDL_3 with chymase at any incubation time point.

A clearly detectable broad band in the molecular mass of approximately 10 kDa appeared in Coomassie Blue-

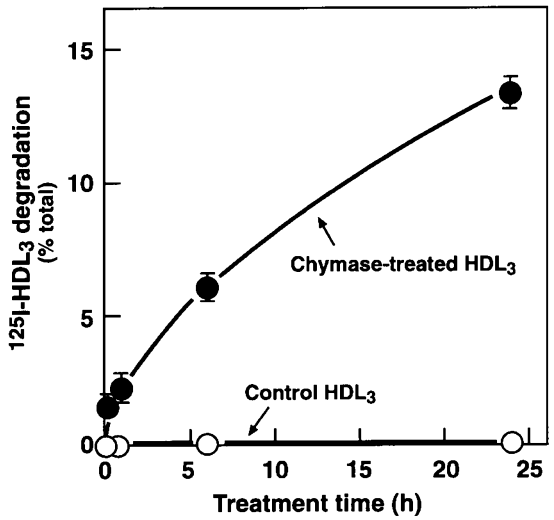

Fig. 1. ^{125}I-HDL_3 (1 mg/mL, 200 cpm/μg) was incubated at 37°C in 1 mL of 150 mM NaCl, 1 mM EDTA, 5 mM Tris-HCl, pH 7.4, in the absence or presence of granule remnants (30 μg total protein equal to 40 BTEE units of chymase). After the indicated periods of time, the incubations were stopped by adding TCA, and the TCA-soluble radioactivity was measured and expressed as a percentage of the total radioactivity present in ^{125}I-HDL_3 at the start of incubation. The TCA-soluble radioactivity of the non-incubated ^{125}I-HDL_3 preparation was 1.3% and it was subtracted from the actual values. Values are means ± SD of triplicate incubations.

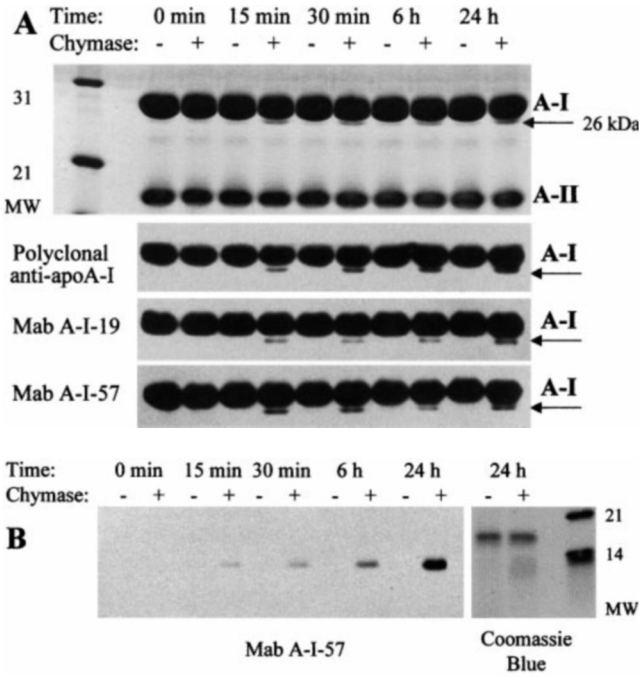

Fig. 2. One milligram of HDL_3 was incubated at 37°C in 1 mL of 150 mM NaCl, 1 mM EDTA, 5 mM Tris-HCl, pH 7.4, in the absence or presence of granule remnants (30 μg total protein equal to 40 BTEE units of chymase) for different periods of time up to 24 h. The incubations were stopped by centrifugation at 15,000 rpm for 5 min, and aliquots of the supernatants were analyzed by SDS-PAGE (15%). After electrophoresis, the peptide bands in the gels were either visualized with Coomassie Blue (uppermost gel) or blotted onto nitrocellulose membranes. The membranes were subjected to immunoblotting with anti-human apoA-I polyclonal antibody, Mab A-I-19, or Mab A-I-57. Apparent molecular masses were calculated using broad-range molecular mass protein standards. Panel A: shows the time course of the reaction of the 26 kDa band with the anti-apoA-I antibodies. Panel B: shows the immunoblot with Mab A-I-57 of the low molecular weight fragments of apoA-I after prolonged incubation with chymase.

stained gels after 24 h of incubation of HDL_3 (Fig. 2, panel B; right). Similar to the large 26 kDa fragment, this band reacted with Mab A-I-57 (panel B; left) and also with Mab A-I-9 and with Mab A-I-19 (not shown) after 15 min of incubation with chymase. These results indicated that these fragments of medium size had been produced by cleavages in the central region of apoA-I. However, long exposure times in autoradiography were necessary, reflecting the small quantity of the peptides.

We next tested, by size exclusion chromatography, whether chymase treatment had modified the size distribution of the HDL_3 particles. Fractionation of native HDL_3 in a Superose 12 column demonstrated the presence of a main peak I (**Fig. 3, panel A**; control HDL_3 (0 min)) which had α electrophoretic mobility in agarose gels (panel B; control HDL_3 (0 min): peak I) followed by a minor peak II corresponding to another group of protein-containing particles of smaller size. Analysis of the electrophoretic mobility of peak II revealed the presence of components with preβ mobility (panel B; control HDL_3 (0 min): peak II), as also reported in previous studies (37).

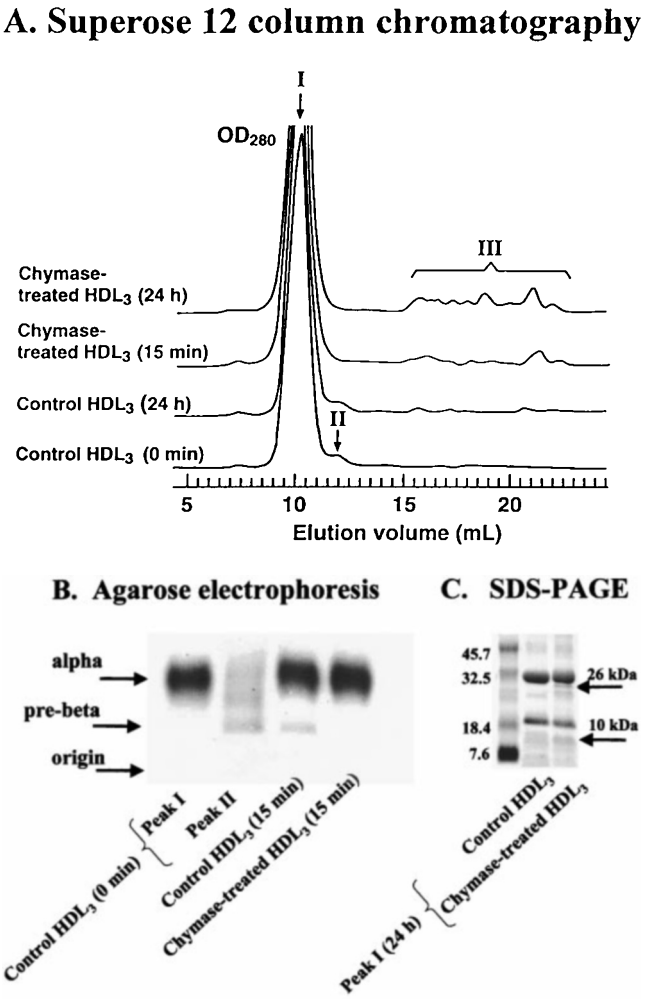

Fig. 3. A: Aliquots of the supernatants described in Fig. 2 containing 150–200 μg of protein from native HDL_3, were applied to Superose 12HR 10/30 gel filtration column and the effluent was monitored at 280 nm. Main fractions are labeled as peaks I, II, and III, respectively. Elution profiles for native HDL_3 (control HDL_3 (0 min)), HDL_3 incubated in the absence of chymase for 24 h (control HDL_3 (24 h)), and HDL_3 incubated with chymase for 15 min or for 24 h (chymase-treated HDL_3) are shown, as indicated. B: Electrophoresis in agarose gels of supernatants described in Fig. 2 corresponding to HDL_3 incubated for 15 min in the absence of chymase (control HDL_3) or the presence of chymase (chymase-treated HDL_3), and peaks I and II obtained by gel filtration of native HDL_3 (control HDL_3 (0 min)). The bands were visualized with Coomassie Blue: origin, and preβ and α regions are labeled. C: SDS-PAGE 15% gel of material eluted in peak I after gel filtration in Superose 12 column of the supernatants described in Fig. 2, and corresponding to HDL_3 after incubation for 24 h in the absence of chymase (control HDL_3) or the presence of chymase (chymase-treated HDL_3). The bands were visualized with Coomassie Blue.

The material eluting in peak II and migrating in preβ position, also contained apoA-I, as demonstrated by immunoblotting. However, the present gel filtration system did not allow the preparative isolation of this minor fraction without its being contaminated with material eluted in peak I. The elution profile of HDL_3 was stable; no change was observed in spite of prolonged incubation of the HDL_3 at 37°C (panel A; control HDL_3 (24 h)). Nota-

bly, treatment of HDL_3 with chymase for only 15 min fully deleted the second peak without affecting the elution profile of the major peak (panel A; chymase-treated HDL_3 (15 min)). Agarose gel electrophoresis of such HDL_3 showed depletion of the preβ-migrating particles (panel B; compare control HDL_3 (15 min) and chymase-treated HDL_3 (15 min)). Finally, already after 15 min of incubation, small peptides (in the MW range of 7–1.3 kDa, and below) were detected in larger elution volumes and were pooled as peak III. Phospholipid analysis of this fraction revealed that the peptides were devoid of this class of lipid. Such "small lipid-free peptides" were not found in control incubations containing only granule remnants (not shown), identifying them as digestion products of apoA-I. Interestingly, even treatment of HDL_3 for 24 h with granule remnant chymase failed to produce any change in the integrity of the α-migrating particles which eluted in peak I (panel A; chymase-treated HDL_3 (24 h)), which remained stable in terms of size, although more of the small lipid-free peptides (peak III) were found than at 15 min. Since proteolysis with chymase did not modify the integrity of the main (α-) lipoprotein species in HDL_3, and only small lipid-free peptides were found to elute separately from the main peak of particles, retention in the α-migrating HDL of the large and medium-sized digestion products (found by SDS-PAGE of the chymase-treated HDL_3 preparation) would explain the surface stability of the α-particles, with prevention of surface-to-core imbalances. To obtain information on the protein profile of the αHDL after proteolysis, we next analyzed by SDS-PAGE the α-migrating particles which eluted in peak I after treatment of the HDL_3 preparation with chymase for 24 h. This analysis revealed that, in fact, both large and medium-sized digestion fragments of apoA-I had remained associated with the αHDL (Fig. 3, panel C).

Recognition of apoA-I in chymase-treated HDL_3 by anti-apoA-I Mabs

Using the set of eight Mabs known to react with various structural domains of apoA-I mainly localized in the central part of the apolipoprotein, we compared their binding to apoA-I in aliquots of HDL_3 that had been incubated with granule remnant chymase for different time intervals (0 min, 15 min, 30 min, 6 h, and 24 h). **Figure 4** shows the results for 3 Mabs at 0 min, 30 min, and 24 h. A striking and rapid reduction was observed in the binding of A-I-9 (epitope between residues 137 and 144 in apoA-I) to chymase-treated HDL_3 at the earliest incubation time (15 min, not shown), and the decline then continued (30 min and 24 h; upper panel). The results with A-I-15 revealed that the region between amino acid residues 93 and 99 was also highly susceptible to be modified by chymase degradation, as binding of this Mab to chymase-treated HDL_3 also started to decline as little as 15 min after the start of incubation (not shown), and after incubation with chymase for 30 min and 24 h the treated HDL_3 reacted more weakly with the antibody (middle panel). In contrast, binding of A-I-11, which recognizes a discontinuous domain in apoA-I between residues 124–128 and 144–148

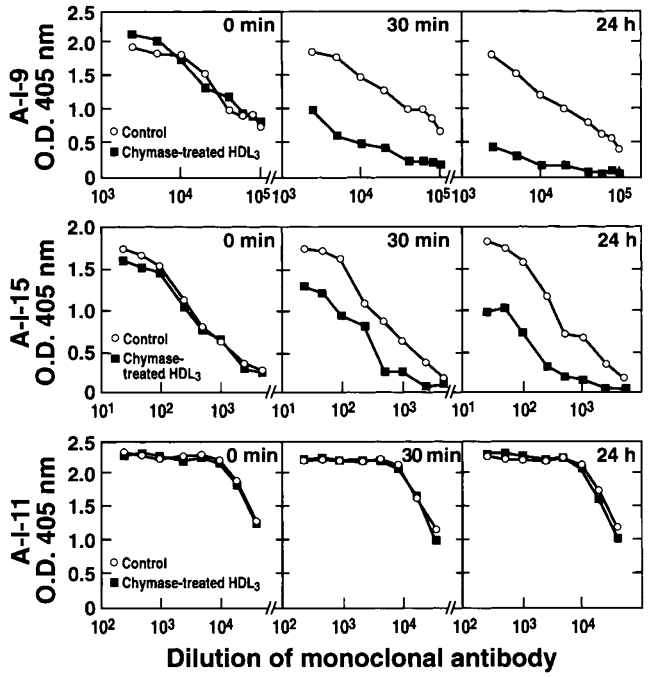

Fig. 4. Aliquots of the supernatants described in Fig. 2 were used to study the binding of A-I-9 (amino acids 137–144) (upper panel), of A-I-15 (amino acids 93–99) (middle panel), and of A-I-11 (discontinuous for residues 124–128 and 144–148 minor) (lower panel) to control and chymase-treated HDL_3 by ELISA, as explained in Methods. Data shown are representative of four parallel experiments.

(minor) to the apoA-I in chymase-treated HDL_3 was not lost even after prolonged incubation (24 h; lower panel). **Figure 5** shows the results obtained with the panel of eight Mabs at all incubation times. The results are expressed as relative values, i.e., for each Mab as a percentage of the binding to HDL_3 that was incubated for a similar time interval in the absence of chymase. The differential sensitivity of binding to chymase-treated HDL_3 is apparent. As shown in Fig. 4 using absolute values, major changes were observed in the binding of A-I-9 to chymase-treated HDL_3, followed by weaker changes in that of A-I-15. After incubation for 15 min, the reduction in A-I-9 binding was already striking, and after incubation for 30 min the binding was reduced by 70%. Similarly, binding of A-I-15 to chymase-treated HDL_3 was reduced by 50% after proteolysis for 30 min. Other central domains of apoA-I also seemed to be modified by the proteolytic action of chymase, but less rapidly. Thus, the relative binding values of A-I-8 and A-I-16 with HDL_3 treated with chymase for 30 min were slightly reduced; they showed 30% reduction with HDL_3 treated for 6 h and a slight further reduction with HDL_3 treated for 24 h. Binding of A-I-19 (residues 1–10) was steadily reduced as treatment time increased, and binding of A-I-57 was only reduced after 6 h, both being reduced by 50% only after prolonged treatment (for 24 h). In contrast, binding of A-I-11 remained completely unchanged, and of A-I-5 almost unchanged at all stages of degradation of HDL_3.

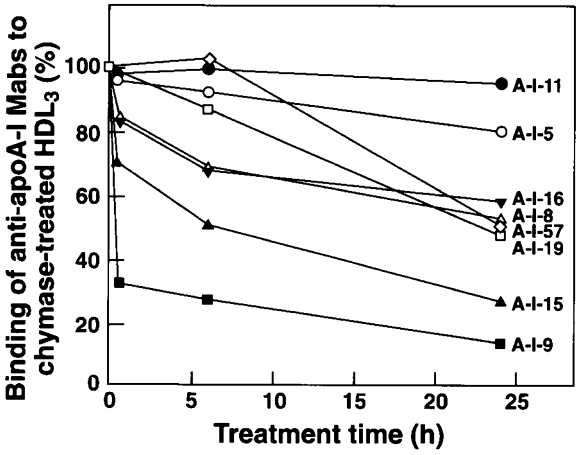

Fig. 5. Aliquots of the supernatants described in Fig. 2, were used to study the binding of a set of eight Mabs to control and chymase-treated HDL_3 by ELISA, as detailed in Methods. The values are expressed as percentages of binding of each Mab to control HDL_3 (time 0 of incubation with chymase) at the antibody dilution which demonstrated the respective 50% reduction in binding.

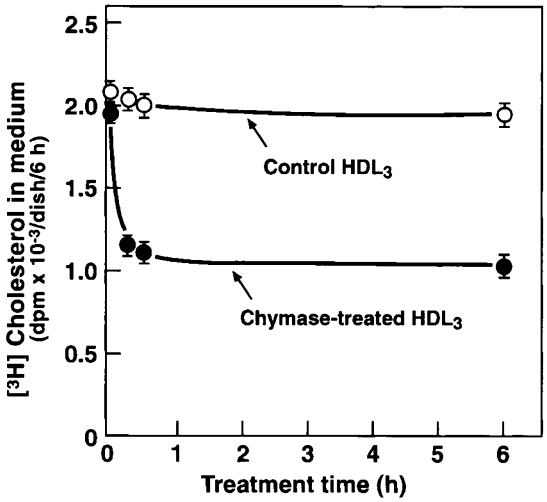

Fig. 6. HDL_3 was preincubated with granule remnants under the conditions described in Fig. 2. The incubations were stopped by sedimenting the granule remnants at 15,000 rpm for 5 min and aliquots of the supernatants were added to ^{3}H-cholesterol-loaded macrophage foam cells at a final concentration of 50 μg/mL of HDL_3 in medium A. The ^{3}H radioactivity of the medium was determined after incubation for 6 h at 37°C. Values are means ± SD of triplicate wells.

Effect of chymase treatment on cholesterol efflux from macrophage foam cells induced by HDL_3

We incubated HDL_3 with granule remnant chymase for 15 min, 30 min, and 6 h, i.e., up to the time period when a major reduction in the chymase-induced inhibition of the binding ability of Mabs to apoA-I had occurred, and tested the ability of the proteolyzed HDL_3 to induce cholesterol efflux from macrophage foam cells. We observed that the shortest incubation with chymase (15 min), which had produced only 1.6% of TCA-soluble degradation products from HDL_3 but 70% loss of binding of Mab A-I-9, an antibody that is specific for an epitope in preβ_1HDL (see Figs. 1 and 4), led to a 60% reduction in the efflux of cholesterol (**Fig. 6**). When the treatment time was prolonged to 6 h, no further reduction was observed, showing that the protease-sensitive efflux activity was fully blocked during the first 15 min of the incubation. In parallel control samples using HDL_3, which had been incubated at 37°C in the absence of granule remnants for the selected periods of time, no such loss of the cholesterol efflux-inducing ability of HDL_3 was observed.

Effect of chymase on LCAT activation by apoA-I in HDL_3

Since a minor degradation of apoA-I was able to reduce the ability of HDL_3 to promote efflux of cholesterol, we performed experiments to evaluate whether proteolytic modification by chymase was also able to alter the second important biological function of HDL in reverse cholesterol transport, i.e., to act as an activator of LCAT. Indeed, proteolysis of HDL_3 by chymase reduced the binding of several Mabs which recognize epitopes in apoA-I involved in the activation of LCAT (see Table 1 and Fig. 5). We then tested the ability of apoA-I in HDL_3 treated with chymase for different time intervals to activate LCAT by measuring the esterification of cholesterol induced by the proteolyzed HDL_3. Unexpectedly, as shown in **Table 2**, no changes in the rates of cholesterol esterification were observed after extensive degradation of HDL_3 with chymase (for 6 h) when 14% of apoA-I had been degraded, and the binding of Mabs A-I-5, A-I-8, and A-I-16 to their respective epitopes on apoA-I was impaired.

DISCUSSION

To gain further insight into the impact of chymase, the major serine protease of mast cells, on the structural and functional modification of apoA-I in HDL, we studied the time course of the proteolysis of apoA-I, and the ability of a set of eight Mabs to recognize specific regions in apoA-I after degradation of HDL_3 by granule remnant chymase.

TABLE 2. Cholesterol esterification activity by LCAT promoted by apoA-I in chymase-treated HDL_3

Incubation Time	Cholesterol Esterification	
	Control HDL_3	HDL_3 Treated
h	*%*	
0	18.3	19.9
0.25	20.2	22.4
0.50	17.6	23.3
6	18.5	20.0

Supernatants of the samples described in Fig. 2 were used for the cholesterol esterification assay. Aliquots of HDL_3 preparations containing 4 μg of cholesterol were taken to determine the cholesterol esterification activity of LCAT in the presence of apoA-I in control and chymase-treated HDL_3, as described in Methods. The cholesterol esterification activity is expressed as the percentage of radioactivity in cholesteryl esters related to the total (free and esterified) cholesterol radioactivity from TLC plates. Values are means of two experiments. The average value for cholesterol esterification of plasma was 28.9%.

We subsequently compared the observed effects with the ability of apoA-I to promote cholesterol efflux from macrophage foam cells and to activate LCAT.

As chymase has a broad specificity, resembling that of α-chymotrypsin, several sites in apoA-I could be potentially cleaved, including sequences present in all the epitopes tested in the present work. However, using limited proteolysis, we found only one major proteolytic product of apoA-I in the HDL_3 fraction, which led to identification of an early cleavage close to the C-terminus of apoA-I, generating a 26 kDa fragment. This result agrees with other reports, which have shown that limited proteolysis with different enzymes produces N-terminal fragments of apoA-I with molecular masses ranging from 22 to 26 kDa (11, 28, 38, 39). Since both α- and preβ-migrating species of HDL were originally present in the HDL_3 fraction but, shortly after chymase treatment, only α-migrating HDL was detected in agarose gels and size exclusion chromatography, the accessibility of the various segments of the apoA-I sequence to chymase is likely to be different for the different subpopulations of HDL_3. This could reflect differences in specific folding and differential exposure of the hinge regions of apoA-I in the lipid-poor or lipid-rich HDL particles. Thus, it is likely that the rapid increase in small peptides (TCA-soluble fraction) was mostly produced by the rapid degradation of apoA-I in the minor preβHDL population, which is very susceptible to proteolysis (40). Indeed, apoA-I epitopes which are specific for preβ particles were rapidly lost by treatment of HDL_3 with chymase. The most rapid loss of the epitope that is specific for $preβ_1HDL$ (recognized by Mab A-I-9), which was paralleled by rapid loss of the ability of HDL_3 to act as a cellular acceptor, provides corroborating evidence that the specific depletion of these particles is the most remarkable modification in the HDL_3 during chymase-dependent proteolysis (7). From the present data it is also likely that the large and medium-sized apoA-I fragments, which were found to be associated with the αHDL, would be generated from a progressive degradation of the apoA-I molecules bound to the α-migrating particles, so explaining the reduction in the intensity of the apoA-I band in SDS-PAGE gels throughout the course of incubation.

Treatment of HDL_3 with granule remnant chymase modified other epitopes in the central region of apoA-I after more extensive fragmentation of apoA-I had occurred. However, it is possible that the progressive loss of the different epitopes may be not only due to the cleavage of domains but also to the presence of domains that are dependent upon residues in the cleaved sites of apoA-I to produce a three-dimensional antigenic site. Two Mabs for discontinuous epitopes, A-I-11 and A-I-16, displayed a particular behavior. These Mabs bind to the same domain in two antiparallel helices of apoA-I, having only a differential affinity in their binding to one particular sequence (22). However, in contrast to A-I-11, binding of which to apoA-I did not change even after treatment of HDL_3 with chymase for 24 h, binding of A-I-16 to its domain in apoA-I was reduced after 6 h of incubation of HDL_3 with chymase, suggesting differences in the susceptibility to proteolytic modification of sequences located in the two different helices. Similarly, the binding of A-I-8 to its epitope (residues 144–148, i.e., a minor domain in A-I-11 but a major domain in A-I-16) was reduced by 30% after incubation of HDL_3 with chymase for 6 h. These data suggest that the region surrounding the major recognition site of A-I-11 is dominated by protein-protein interactions and is probably associated with a more rigid tertiary structure of apoA-I, making it less susceptible to a change in conformation. Accordingly, the epitope for Mab A-I-5 (amino acids 133–141) located close to the major epitope for Mab A-I-11 (amino acids 124–128) was only mildly modified by chymase proteolysis. The high resistance of the epitope for Mab A-I-11 to proteolytic modification and the proneness of apoA-I to lose its ability to cause cholesterol efflux after a minor degree of proteolysis also suggests that this epitope, which was previously shown not to be involved in the activation of LCAT (22), is not essential for the promotion of cellular cholesterol efflux by HDL_3 either.

The fact that apoA-I, when compared with other apolipoproteins, is a better activator of LCAT has led to the hypothesis that LCAT must interact with a particular domain of this apolipoprotein. Moreover, the finding that apoA-I in αHDL, but not in the $preβ_1HDL$ subpopulation, is able to activate LCAT has focused attention on the specific conformation of apoA-I that is required for this function. Accordingly, several reports deal with the identification of domains in apoA-I that are important for LCAT activation (17–22). The central region of apoA-I between the amino acids 124 and 174 (epitopes recognized by A-I-5, A-I-8, A-I-16, and A-I-57) was shown to be important for LCAT activation (22). Because treatment of HDL_3 with granule remnant chymase modified these epitopes with varying efficiency (see Fig. 5), we tested the possibility that proteolysis of HDL_3 by granule remnants would also alter the ability of apoA-I to activate LCAT. However, even proteolytic modification of HDL_3 by chymase, which causes 14% loss of apoA-I in PAGE gels, failed to decrease the ability of the proteolyzed particles to induce cholesterol esterification via the activity of LCAT. This observation contrasts with another report that blocking of a single epitope in the apoA-I region between amino acids 96 and 111 leads to inhibition of the ability of apoA-I to activate LCAT (18). This apparent paradox could be explained by secondary changes in the conformation of other regions of apoA-I induced by the binding of a single Mab to its epitope, as has been found using Mabs to apoA-I (22) or to apoB-100 (41). Indeed, the present data do not support the hypothesis that a change in a single domain of apoA-I is involved in the conversion of lymphatic preβHDL, without LCAT activation ability, into plasmatic αHDL, which has acquired the LCAT activation capacity. Interestingly, it has been suggested that the high content of sphingomyelin found in lymphatic HDL particles impairs the binding of LCAT to the interface, thus contributing to their low reactivity with LCAT (42). The role of the lipid composition of HDL in modulating the ability of apoA-I to activate LCAT could be attributed to changes induced in the

properties of the lipid interface or to a competing effect for substrate binding, as has been recently reviewed (43).

As loss of integrity of a fraction of apoA-I did not alter the ability of the HDL_3 preparation to activate LCAT, we can infer that, in the present conditions, the fragments produced by chymase proteolysis were also capable of activating LCAT, like intact apoA-I. One explanation is that the large and medium-sized fragments which remained bound to the surface of α-migrating HDL_3 had several amphipathic helices arranged in a conformation suitable for maintaining the LCAT activation properties of the proteolyzed apoA-I. In fact, proteolytic cleavage is likely to occur predominantly in polypeptide segments connecting structural domains (44). Interestingly, limited proteolysis of apoA-I in reconstituted models of HDL with four different proteases has been reported to produce a relatively stable N-terminal polypeptide of approximately 22 kDa which retains the LCAT activation function of apoA-I (38). Indeed, the fact that no mechanism involving the structure of a specific domain in apoA-I and its ability as LCAT co-factor has yet been described, suggests that, rather than specific protein domains, the presence of amphipathic helices is sufficient for activation of LCAT. Moreover, even different synthetic amphipathic peptides and CNBr fragments of apoA-I have been able to activate LCAT with varying efficiencies (45). In support of this concept, it has recently been suggested that salt bridge formation between positive charges in LCAT and negative charges in the amphipathic helices of apoA-I are directly involved in the activation of the enzyme (46). Thus, it is possible that only much stronger modifications of HDL, such as those causing high MW cross-linked forms of apoA-I and apoA-II, would cause inhibition of LCAT activity (47).

In summary, our data indicate that a minimal proteolytic modification of apoA-I leads to rapid disappearance of the epitope which is specific for the minor $preβ_1HDL$ subpopulation, with concurrent loss of the ability to promote high-affinity efflux of cholesterol by the proteolyzed HDL_3, and that modification of several apoA-I epitopes involved in the activation of LCAT does not abolish this function of HDL_3. The data also suggest that amphipathic helical repeats contained in fragments of apoA-I which remain bound to the α-migrating HDL keep this function more resistant to proteolytic inhibition. The very high sensitivity of apoA-I in the $preβ_1HDL$ particles to mast cell chymase suggests that in fatty streak lesions containing both mast cells and foam cells, chymase released from activated mast cells could produce proteolytic cleavage in apoA-I that is critical for the promotion of cellular efflux of cholesterol. This sequence of events could lead to local inhibition of the earliest step of reverse cholesterol transport in the arterial intima, specifically in fatty streak areas in which the number of degranulated mast cells is increased (48).

In the present study, proteolysis of HDL by mast cell chymase turned out to be a suitable tool for studying structure–function relationships in HDL. Such studies may also contribute to the identification and characterization of areas of apoA-I that are dominated by protein–protein interactions and are less susceptible to proteolytic cleavage. This model of proteolytically modified HDL could be extended to other relevant proteases also found in atherosclerotic lesions, such as mast cell tryptase, thrombin, and plasmin. Whether proteolytic modification of epitopes in apoA-I could also alter other biological functions of apoA-I, such as its interactions with cholesteryl ester transfer protein and phospholipid transfer protein, remains to be studied.

This project was supported by a grant from the Sigrid Juselius Foundation to M. Lee, and by a grant from the Ministero Pubblica Istruzione to A. L. Catapano.

Manuscript received 16 September 1999 and in revised form 15 February 2000.

REFERENCES

1. Barter, P. J., and K-A. Rye. 1996. High density lipoproteins and coronary heart disease. *Atherosclerosis.* **121:** 1–12.
2. Fielding, C. F., and P. E. Fielding. 1995. Molecular physiology of reverse cholesterol transport. *J. Lipid Res.* **36:** 211–228.
3. von Eckardstein, A., A. Y. Huang, and G. Assman. 1994. Physiological role and clinical relevance of high-density lipoprotein subclasses. *Curr. Opin. Lipidol.* **5:** 404–416.
4. Castro, G. R., and C. J. Fielding. 1988. Early incorporation of cell-derived cholesterol into pre-β-migrating high density lipoprotein. *Biochemistry.* **27:** 25–29.
5. Lee, M., L. Lindstedt, and P. T. Kovanen. 1992. Mast cell-mediated inhibition of reverse cholesterol transport. *Arterioscl. Thromb. Vasc. Biol.* **12:** 1329–1335.
6. Lindstedt, L., M. Lee, G. R. Castro, J-C. Fruchart, and P. T. Kovanen. 1996. Chymase in exocytosed rat mast cell granules effectively proteolyzes apolipoprotein AI-containing lipoproteins, so reducing the cholesterol efflux-inducing ability of serum and aortic intimal fluid. *J. Clin. Invest.* **97:** 2174–2182.
7. Lee, M., A. von Eckardstein, L. Lindstedt, G. Assmann, and P. T. Kovanen. 1999. Depletion of $preβ_1$LpA-I and LpA-IV by mast cell chymase reduces the cholesterol efflux ability promoted by plasma. *Arterioscler. Thromb. Vasc. Biol.* **19:** 1066–1074.
8. Brouillette, C. G., and G. M. Anantharamaiah. 1995. Structural models of apolipoprotein A-I. *Biochim. Biophys. Acta.* 1256: 103–129.
9. Palgunachari, M. N., V. K. Mishra, S. Lund-Katz, M. C. Phillips, S. O. Adeyeye, S. Alluri, G. M. Anantharamaiah, and J. P. Segrest. 1996. Only the two end helixes of eight tandem amphipathic helical domains of human apoA-I have significant lipid affinity. Implications for HDL assembly. *Arterioscler. Thromb. Vasc. Biol.* **16:** 328–338.
10. Allan, C. M., N. H. Fidge, J. R. Morrison, and J. Kanellos. 1993. Monoclonal antibodies to human apolipoprotein AI: probing the putative receptor binding domain of apolipoprotein AI. *Biochem. J.* **290:** 449–455.
11. Dalton, M. B., and J. B. Swaney. 1993. Structural domains of apolipoprotein A-I within high density lipoproteins. *J. Biol. Chem.* **268:** 19274–19283.
12. Luchoomun, J., N. Theret, V. Clavey, P. Duchateau, M. Rosseneu, R. Brasseur, P. Denefle, J-C. Fruchart, and G. R. Castro. 1994. Structural domain of apolipoprotein A-I involved in its interaction with cells. *Biochim. Biophys. Acta.* **1212:** 319–326.
13. Davidson, W. S., S. Lund-Katz, W. J. Johnson, G. M. Anantharamaiah, M. N. Palgunachari, J. P. Segrest, G. H. Rothblat, and M. C. Phillips. 1994. The influence of apolipoprotein structure on the efflux of cellular free cholesterol to high density lipoprotein. *J. Biol. Chem.* **269:** 22975–22982.
14. Banka, C. L., A. S. Black, and L. K. Curtiss. 1994. Localization of an apolipoprotein A-I epitope critical for lipoprotein-mediated cholesterol efflux from monocytic cells. *J. Biol. Chem.* **269:** 10288–10297.
15. Fielding, P. E., M. Kawano, A. L. Catapano, A. Zoppo, S. Marcovina, and C. J. Fielding. 1994. Unique epitope of apolipoprotein A-

I expressed in pre-β-1 high density lipoprotein and its role in the catalyzed efflux of cellular cholesterol. *Biochemistry.* **33:** 6981–6985.
16. Sviridov, D., L. Pyle, and N. Fidge. 1996. Identification of a sequence of apolipoprotein A-I associated with the efflux of intracellular cholesterol to human serum and apolipoprotein A-I containing particles. *Biochemistry.* **35:** 189-196.
17. Banka, C. L., D. J. Bonnet, A. S. Black, R. S. Smith, and L. K. Curtiss. 1991. Localization of an apolipoprotein A-I epitope critical for activation of lecithin-cholesterol acyltransferase. *J. Biol. Chem.* **266:** 23886–23892.
18. Wong, L., L. K. Curtiss, J. Huang, C. J. Mann, B. Maldonado, and P. S. Roheim. 1992. Altered epitope expression of human interstitial fluid apolipoprotein A-I reduces its ability to activate lecithin cholesterol acyl transferase. *J. Clin. Invest.* **90:** 2370–2375.
19. Minnich, A., X. Collet, A. Roghani, C. Cladaras, R. L. Hamilton, C. J. Fielding, and V. I. Zannis. 1992. Site-directed mutagenesis and structure-function analysis of the human apolipoprotein A-I. *J. Biol. Chem.* **267:** 16553–16560.
20. Meng, Q-H., L. Calabresi, J-C. Fruchart, and Y. L. Fruchart. 1993. Apolipoprotein A-I domains involved in the activation of lecithin:cholesterol acyltransferase. *J. Biol. Chem.* **268:** 16966–16973.
21. Sorci-Thomas, M., M. W. Kearns, and J. P. Lee. 1993. Apolipoprotein A-I domains involved in lecithin-cholesterol acyltransferase activation. Structure:function relationships. *J. Biol. Chem.* **268:** 21403–21409.
22. Uboldi, P., M. Spoladore, S. Fantappie, S. Marcovina, and A. L. Catapano. 1996. Localization of apolipoprotein A-I epitopes involved in the activation of lecithin:cholesterol acyltransferase. *J. Lipid Res.* **37:** 2557–2568.
23. Lindstedt, K. A., J. O. Kokkonen, and P. T. Kovanen. 1992. Soluble heparin proteoglycans released from stimulated mast cells induce uptake of low density lipoproteins by macrophages via scavenger receptor-mediated phagocytosis. *J. Lipid Res.* **33:** 65–75.
24. Lowry, O. H., N. J. Rosebrough, A. L. Farr, and R. J. Randall. 1951. Protein measurement with Folin phenol reagent. *J. Biol. Chem.* **193:** 265–275.
25. Woodbury, R. G., M. T. Everitt, and H. Neurath. 1981. Mast cell proteases. *Methods Enzymol.* **80:** 588–609.
26. Kokkonen, J. O., M. Vartiainen, and P. T. Kovanen. 1986. Low density lipoprotein degradation by secretory granules of rat mast cells. *J. Biol. Chem.* **261:** 16067–16072.
27. Havel, R. J., H. A. Eder, and J. H. Bragdon. 1955. The distribution and chemical composition of ultracentrifugally separated lipoproteins in human serum. *J. Clin. Invest.* **34:** 1345–1353.
28. Lindstedt, L., J. Saarinen, N. Kalkkinen, H. Welgus, and P. T. Kovanen. 1999. Matrix metalloproteinases −3, −7, and −12, but not −9, reduce high density lipoprotein-induced cholesterol efflux from human macrophage foam cells by truncation of the carboxyl terminus of apolipoprotein AI. *J. Biol. Chem.* **274:** 22627–22634.
29. Basu, S. K., Goldstein J. L., Anderson R. G. W., and Brown M. S. 1976. Degradation of cationized low density lipoprotein and regulation of cholesterol metabolism in homozygous familial hypercholesterolemia fibroblasts. *Proc. Natl. Acad. Sci. USA.* **73:** 3178–3182.
30. Brown, M. S., S. E. Dana, and J. L. Goldstein. 1975. Receptor-dependent hydrolysis of cholesteryl esters contained in plasma low density lipoprotein. *Proc. Natl. Acad. Sci. USA.* **72:** 2925–2929.
31. McFarlane, A. S. 1958. Efficient trace-labeling of proteins with iodine. *Nature (London)* **182:** 53–57.
32. Bilheimer, D. W., S. Eisenberg, and R. I. Levy. 1972. The metabolism of very low density lipoproteins. I. Preliminary in vitro and in vivo observations. *Biochim. Biophys. Acta.* **260:** 212–221.
33. Weber, K., and M. Osborn. 1969. The reliability of molecular weight determination by dodecyl sulfate polyacrylamide gel electrophoresis. *J. Biol. Chem.* **244:** 4406–4412.
34. Towbin, H., T. Staehelin, and J. Gordon. 1979. Electrophoretic transfer of proteins from polyacrylamide gels to nitrocellulose sheets: procedure and some applications. *Proc. Natl. Acad. Sci. USA.* **76:** 4350–4354.
35. Chen, C-H., and J. J. Albers. 1985. A rapid large-scale procedure for purification of lecithin-cholesterol acyltransferase from human and animal plasma. *Biochim. Biophys. Acta.* **834:** 188–195.
36. Albers, J. J., C-H. Chen, and A. G. Lacko. 1986. Isolation, characterization, and assay of lecithin cholesterol acyltransferase. *Methods Enzymol.* **129:** 763–783.
37. Clay, M. A., and P. J. Barter. 1996. Formation of new HDL particles from lipid-free apolipoprotein A-I. *J. Lipid. Res.* **37:** 1722–1732.
38. Ji, Y., and A. Jonas. 1995. Properties of an N-terminal proteolytic fragment of apolipoprotein AI in solution and in reconstituted high density lipoproteins. *J. Biol. Chem.* **270:** 11290–11297.
39. Roberts, L. M., M. J. Ray, T-W. Shih, E. Hayden, M. M. Reader, and C. G. Brouillette. 1997. Structural analysis of apolipoprotein A-I: Limited proteolysis of methionine-reduced and -oxidized lipid-free and lipid-bound human apoA-I. *Biochemistry.* **36:** 7615–7624.
40. Kunitake, S. T., G. Ch. Chen, S-F. Kung, J. W. Schilling, D. A. Hardman, and J. P. Kane. 1989. Pre-beta high density lipoprotein. Unique disposition of apolipoprotein A-I increases susceptibility to proteolysis. *Arteriosclerosis.* **10:** 25–30.
41. Fantappie, S., A. Corsini, A. Sidoli, S. Marcovina, P. Uboldi, A. Granata, B. Da Ros, P. Rossi, R. Fumagalli, and A. L. Catapano. 1992. Monoclonal antibodies to human low density lipoprotein identify distinct areas on apolipoprotein B-100 relevant to the LDL-receptor interaction. *J. Lipid Res.* **33:** 1111–1121.
42. Bolin, D. J., and A. Jonas. 1996. Sphingomyelin inhibits the lecithin-cholesterol acyltransferase reaction with reconstituted high density lipoproteins by decreasing enzyme binding. 1996. *J. Biol. Chem.* **271:** 19152–19158.
43. Jonas, A. 1998. Regulation of lecithin cholesterol acyltransferase activity. *Prog. Lipid Res.* **37:** 209–234.
44. Wilson, J. E. 1991. The use of monoclonal antibodies and limited proteolysis in elucidation of structure-function relationships in proteins. *Methods Biochem. Anal.* **35:** 207–250.
45. Vanloo, B., J. Taveirne, J. Baert, G. Lorent, L. Lins, J. M. Ruyschaert, and M. Rosseneu. 1992. LCAT activation properties of apoA-I CNBr fragments and conversion of discoidal complexes into spherical particles. *Biochim. Biophys. Acta.* **1128:** 258–266.
46. Wang, J., J. A. Delozie, A. K. Gevre, P. J. Dolpin, and J. S. Parks. 1998. Role of glutamic acid residues 154, 155, and 165 of lecithin:cholesterol acyl transferase in cholesterol esterification and phospholipase A2 activities. *J. Lipid Res.* **39:** 51–58.
47. McCall, M. R., J. J. M. van den Berg, F. A. Kuypers, D. L. Tribble, R. M. Krauss, L. J. Knoff, and T. M. Forte. 1994. Modification of LCAT activity and HDL structure. New links between cigarette smoke and coronary heart disease risk. *Arterioscler. Thromb. Vasc. Biol.* **14:** 248–253.
48. Kaartinen, M., A. Penttilä, and P. T. Kovanen. 1995. Extracellular mast cell granules carry apolipoprotein B-100-containing lipoproteins into phagocytes in human arterial intima. Functional coupling of exocytosis and phagocytosis in neighboring cells. *Arterioscler. Thromb. Vasc. Biol.* **15:** 2047–2054.